

**ULTRA-REFRACTORY CALCIUM-ALUMINUM-RICH INCLUSION IN AN AOA IN CR CHONDRITE YAMATO-793261.** M. Komatsu<sup>1,2</sup>, T. J. Fagan<sup>2</sup>, A. Yamaguchi<sup>1,3</sup>, T. Mikouchi<sup>4</sup>, M. Yasutake<sup>1,3</sup>, and M. E. Zolensky<sup>5</sup>, <sup>1</sup>SOKENDAI, Graduate University for Advanced Studies, Kanagawa, Japan (komatsu\_mutsumi@soken.ac.jp), <sup>2</sup>Dept. Earth Sciences, Waseda University, Japan, <sup>3</sup>National Institute of Polar Research, Japan, <sup>4</sup>Dept. Earth and Planetary Science, University of Tokyo, Japan, <sup>5</sup>ARES, NASA Johnson Space Center, Houston, USA.

**Introduction:** CR chondrites are a group of primitive carbonaceous chondrites that preserve nebular records of the formation conditions of their components [e.g., 1;2]. We have been investigating a set of Antarctic CR chondrites from the Japanese-NIPR collection in order to study variations within this group. During our study, we have found an AOA that encloses an ultrarefractory (UR) CAI in Yamato-793261 (Y-793261). UR CAIs are rare in carbonaceous chondrites [e.g., 3], and only three UR CAIs in AOAs have been identified so far [3-5]. UR CAIs can provide information on crystallization processes at very high temperatures in the solar nebula. Here we describe the petrology of Y-793261, and preliminary results on this newly discovered AOA enclosing a UR CAI.

**Methods:** A polished thin section of Y-793261 was studied using SEM, EPMA, and Raman spectroscopy. Petrology and Raman characteristics are also compared to those from other CR chondrites and the primitive CO chondrite Y-81020, as listed in Table 1.

Imaging, mineral identification and quantitative analyses were performed using a JEOL JSM-7100F FE-SEM and JEOL JXA8200 EPMA at NIPR. Our Zr analyses may have been affected by an interference of Sc on Zr L $\alpha$ . We plan to determine the magnitude of this interference in future work, but the ZrO<sub>2</sub> data reported here are uncorrected and should be considered preliminary. Raman spectra were collected using a JASCO NRS-1000 Raman Spectrometer at NIPR. Raman analytical parameters were similar to those of [6].

## Results and Discussion:

### Petrography of Y-793261

CR chondrite Y-793261 is composed of chondrules, AOAs, CAIs, mineral fragments, and matrix. AOAs and CAIs are more abundant in Y-793261 than in other CR chondrites we have examined; eight AOAs are present in the Y-793261 thin section, whereas the other CR thin sections have only 0 to 2 AOAs (Table 1).

Previous work has shown that aqueous alteration in CR chondrites causes (1) variable replacement of metallic Fe-Ni by magnetite or sulfide and (2) formation of phyllosilicates along edges, fractures and twin boundaries of olivine and pyroxene [11]. In Y-793261, phyllosilicates occur in matrix and around some chondrules, but are rare inside chondrules. The minimal alteration of mafic phenocrysts suggests that Y-793261

is similar to weakly altered petrologic types 2.6-2.5 described in [11].

### Maturation grade of organic material in Y-793261

Raman spectra were collected on randomly-selected matrix areas in thin sections. Raman spectra from CR chondrites in this study exhibit first-order carbon D- and G-bands at ~1350 and ~1600 cm<sup>-1</sup> respectively.

[6], [12] and [13] showed that I<sub>d</sub>/I<sub>g</sub> increases in petrologic type from 3.0 to 3.7 in CO/CV and unequilibrated ordinary chondrites (UOCs). Because the compositions of organic matter in CR and CV/CO are similar, Raman parameters can be used for interclass comparison to compare their metamorphic grades. The spectra collected for this study from CR chondrites including Y-793261 all show relatively low I<sub>d</sub>/I<sub>g</sub>, suggesting low thermal maturity, particularly in comparison with matured UOCs and CV chondrites (P.T.>3.6) (Fig. 1).

### High temperature signature of AOA:

Eight AOAs are found in the thin section of Y-793261. All AOAs in Y-793261 show little evidence for secondary aqueous alteration or thermal alteration.

AOA #4 consists mostly of fine-grained olivine, which often encloses segregations of Al-diopside and anorthite in a texture typical of AOAs (Fig. 2c). In one of these segregations, Al-diopside is in contact with Sc-rich pyroxene and a Zr-rich phase, similar to Sc-Zr-rich phases observed previously in UR CAIs [e.g., 3]. The UR inclusion has a concentric texture with a Zr,Sc-rich pyroxene core surrounded by Sc-rich pyroxene.

Refractory high-Ca pyroxenes in AOA #4 contain 17-36 wt.% Al<sub>2</sub>O<sub>3</sub> and 6-10 wt.% TiO<sub>2</sub>. The high Al-contents suggest that tiny inclusions of corundum or another Al-rich phase may be present. Concentrations of Sc<sub>2</sub>O<sub>3</sub> and ZrO<sub>2</sub> (uncorrected for possible interference) vary between 2 and 8 wt.% and are positively correlated, increasing from core to rim (Fig. 3a). These Sc<sub>2</sub>O<sub>3</sub> and ZrO<sub>2</sub> concentrations in pyroxene are intermediate between higher and lower values identified in previous studies of several UR CAIs [3] (Fig. 3). Pyroxene from UR CAI 3N-24 from oxidized CV chondrite NWA 3118 has a range of ZrO<sub>2</sub> concentrations similar to that of AOA #4, but with lower Sc<sub>2</sub>O<sub>3</sub> [3] (Fig. 3b). The presence of the UR inclusion indicates that condensation of AOA #4 started at higher temperature than other AOAs in CR chondrites.

### Enrichment of SiO<sub>2</sub> at lower temperature:

AOA #4 also contains ~5  $\mu$ m sized, nearly pure SiO<sub>2</sub> grains with low-Ca pyroxene grains (Fig. 2d). It is not

clear whether the SiO<sub>2</sub> is crystalline or amorphous. In previous studies, pod-like SiO<sub>2</sub> grains were found in the chondrule margins in CR chondrite PCA 91082 [15]. [16] found that many Type I chondrules in CR chondrites contain silica-rich igneous rims (SIR), and suggested that SIR are formed either by gas-solid condensation onto chondrule surfaces and subsequent incomplete melting, or by direct condensation of SiO<sub>(v)</sub> into chondrule melts.

We have not observed SiO<sub>2</sub> grains in AOAs prior to this study. SiO<sub>2</sub> grains in AOA #4 occur with low-Ca pyroxene, suggesting formation at temperatures below typical olivine condensation temperatures [17]. AOA #4 in Y-793261 apparently preserves evidence of condensation at unusually high temperature (indicated by the UR CAI), combined with low-T interaction with gas (indicated by SiO<sub>2</sub> + low-Ca pyroxene).

**References:** [1] Weisberg M. K. et al. (1993) *GCA*, 57, 1567-1586. [2] Krot A.N. et al. (2002) *MaPS*, 37, 1451-1490. [3] Ivanova M. A. et al. (2012) *MaPS* 47, 2107-2127. [4] Ma C. et al. (2012) *Am. Min.*, 97, 1219-1225. [5] Noonan A.F. et al. (1977) *Meteoritics*, 12, 332-335. [6] Bonal. L. et al. (2006) *GCA*, 70,1849-1863. [7] Kojima H. and Yamaguchi A. (2005) *Meteorite Newsletter, NIPR*. [8] Schrader D. et al. (2011) *GCA*, 75, 308-325. [9] Davidson J. et al. (2014) *MaPS*, 49, 1456-1474. [10] Fukushima H. (2016) *Masters Thesis, Waseda University*. [11] Harju E.R. et al. (2014) *GCA*, 139, 267-292. [12] Quirico E. et al. (2003) *MaPS*, 38, 795-881. [13] Bonal L. et al. (2007) *GCA*, 71, 1605-1623. [14] El Goersy A. et al. (2002) *GCA*, 66, 1459-1491. [15] Noguchi T. et al. (1995) *Proc. NIPR Symp.*, 8, 33-62. [16] Krot A.N. et al. (2004) *MaPS*, 39,1931-1955. [17] Krot A.N. et al. (2004) *GCA*, 68,1293-1941.

Table 1. Samples used in this study.

Name	Type	No. of AOAs <sup>a</sup>
Y-793261	CR2	8
Y-790112	CR2	not observed
Y-793495	CR2	not observed
Y-8449	CR2	not observed
Y-792518	CR2	not observed
A-881595	CR2(ungrouped C3?) <sup>b</sup>	2
Y-81020	CO3.0	37 <sup>c</sup>

<sup>a</sup>Number of AOAs found in one thin section. <sup>b</sup>A-881595 was originally classified as a CR2 chondrite [7], but re-classification as an ungrouped C3 has been suggested [8,9]. <sup>c</sup>Unpublished data from [10].

➔ Fig. 3. ...from Efremovka, *HIB-11* from Murchison, *OSCAR* from Ornans [3 and references therein].

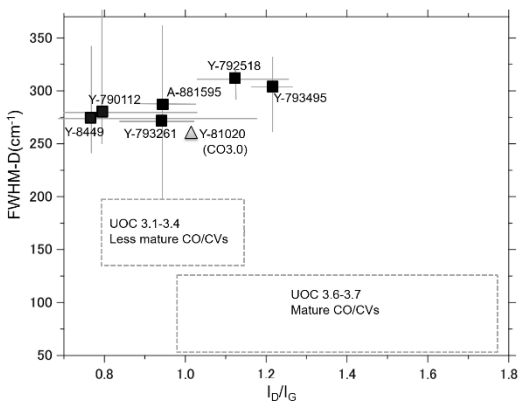


Fig.1. Spectral parameters of Raman bands of OMs in CR chondrites and Y-81020 in this study (after [6,12]).

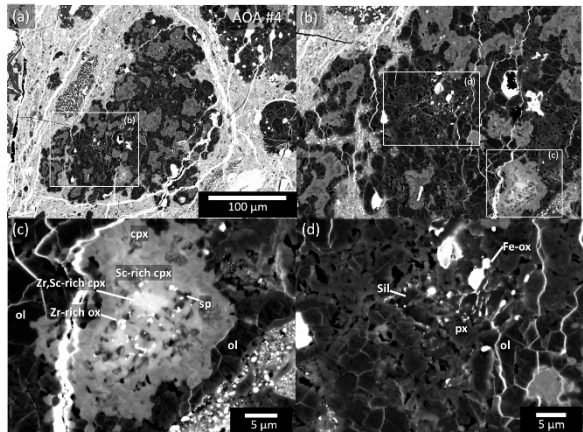


Fig. 2. BSE images of AOA #4. ol=olivine, cpx=high-Ca pyroxene, sp=spinel, Zr-rich ph=Zr-rich phase, Zr, Sc-rich cpx=Zr, Sc-rich high Ca pyroxene.

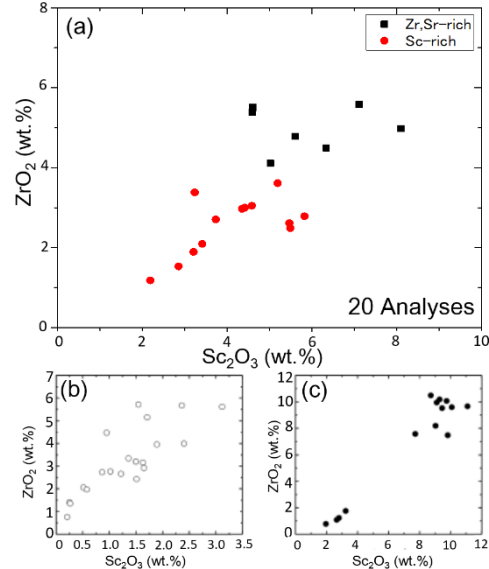


Fig. 3. Uncorrected ZrO<sub>2</sub> and Sc<sub>2</sub>O<sub>3</sub> in pyroxene in UR CAIs from (a) AOA #4 (this study), (b) UR CAI 3N-24 from CV<sub>ox</sub> chondrite NWA 3118 [3] and (c) 33E-1